The investigation on local time dependency of dust storm initiation in the Solis Plunum - the Valles Marineris region

Sho Okuno[1], Kazunori Ogohara[1], 1. Kyoto Sangyo Univ.

Abstract

The Solis Planum - Valles Marineris region is famous for its unique and strong dust activities. They sometimes affect the Martian atmosphere in global scale [1]. In this study, we investigated the occurrence time of dust storms in the region by using the data collected by Emirates eXploration Imager (EXI) onboard HOPE probe. HOPE is orbiting in a near equational orbit and the orbital period is 55h. It can get the picture of the Martian atmosphere on diurnal and sub-seasonal timescales [2]. EXI has several observational wavelengths in ultraviolet and visible bands. We used three kinds of images in visible bands, 437nm, 546nm and 635nm. We visually inspected the images in the region and extracted dust storms. We found 37 storms which we can discuss occurrence times The result suggests that it is likely to occur frequently around LT1200 in the southern winter, and LT0900 in southern spring. We are not able to see the local time dependency in other seasons because of the small number of detected storms.

1. Introduction

From the long-term observation, we know that dust storms occur frequently on Mars. Dust storms are classified into three categories by their scale (Table1). On the contrary, they are also categorized into three types by their texture found in satellite images (Fig1). [5] investigated the spatial and temporal distribution of textured dust storm. However, local time dependency of dust storm initiations was not investigated due to observational limitations caused by the orbit of the satellite. [3] investigated dust storm all regions in MY36. On the contrary, this study focuses on the Solis – Valles Marineris region (Fig3). Because of the interpretation of initial phase of dust storm, they could have estimated the initiation time later. Therefore, we investigate the initiation time more accurately.

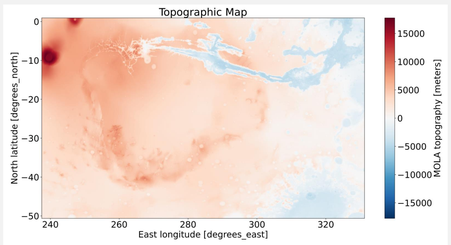

Fig3. The Solis-Marineris region ($50° S \sim 0° S, 240° E \sim 330° E$)

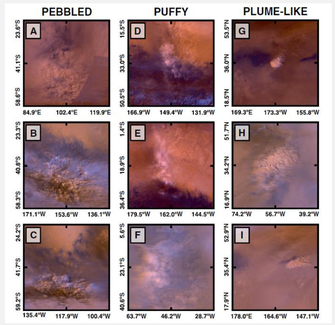

(left) Fig1.
Example images of textured dust storms [5]
(below) Fig2.
Spatial distribution of textured dust storms [5]

Table1.
Classification by scale [4]

	Size	Life Time
Local	10^2 km^2 ~	~ 1 sol
Regional	1.6×10^6 km^2~	2 sol ~
Global	planet-encircling	several month

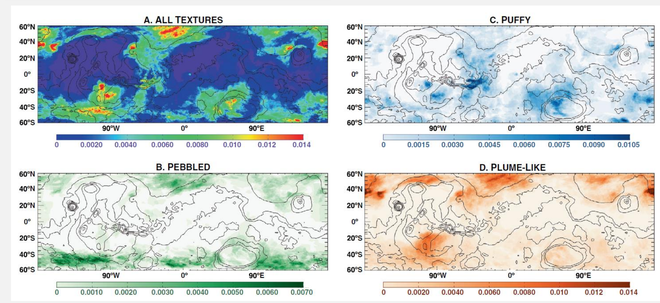

2. Data and Method

We used the data collected by Emirates eXploration Imager (EXI) onboard HOPE probe. HOPE is orbiting in a near equational orbit and the orbital period is 55h. It can get the picture of the Martian atmosphere on diurnal and sub-seasonal timescales [2]. We used L2A images taken by XOS1 observation mode. They are calibrated images and include meta data such as the sub-spacecraft point and photometric angles. EXI has several observational wavelengths in ultraviolet and visible bands. We chose three kinds of images in visible bands, 437nm, 546nm and 635nm. The spatial resolution is 2 ~ 4 km. We used data from $L_s = 6.4°$ in MY 36 to $L_s = 27.0°$ in MY37.

At first, we converted the images into longitudinal and latitudinal coordinates by using the way of [6]. Although the photometric correction used in [7] is for Mars Daily Global Maps (MDGMs), we adopted it to distinguish dust and water ice cloud in EXI images. The processed images are shown in Fig4.

We visually inspected the images in the region and extracted dust storms. The initiation time of dust storms is defined as follows. If consecutive two images capture just before and just after dust storms occur, we define the occurrence time as the time between two images (see Fig5).

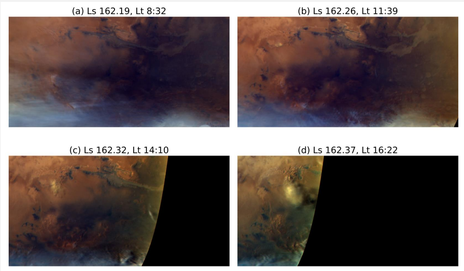

Fig5. The satellite images and time variation of dust storm
In this event, the initiation time is 1000LT, which is between (a) and (b)

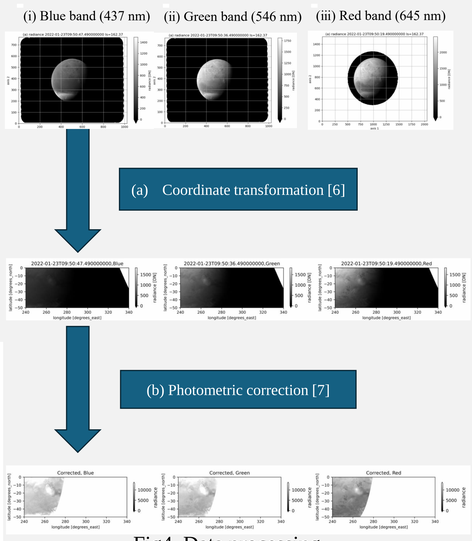

Fig4. Data processing

(Top) EXI XOS1 L2A images
from left, (i) blue, (ii)green, (iii) red band
(Middle) images processed by (a)
(Bottom) images processed by (b)

3. Results and Conclusions

From the images described in 2, we found 37 storms.

At first, we show the seasonal and initiation local time distribution of detected storms in Fig6. From $L_s = 100$ to $L_s = 120$, we could not get any data because of several issues related to spacecrafts which is described in [8]. From $L_s = 308$ to $L_s = 314$, regional dust storm which started from Chryse Planitia ($35° W, 15° N$) and came to the region. 3 storms cannot be distinguished from the larger regional dust storm.

Fig6 suggests that:

A) Few storms were observed in the solstices.
B) No storms occurred after 1700 LT.

A) was consistent with solstitial pause [1]. Fig7(a) shows the seasonal distribution. We define the season by dividing a year by 45° before and after the solstices and the equinoxes. For instance, the southern fall is from $L_s = 0°$ to $L_s = 90°$. Fig7(a) suggests that about 60% occurred in the southern spring.

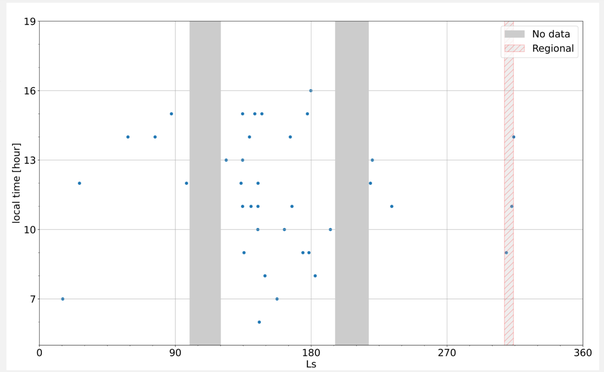

Fig6. A Scatter diagram showing the relationship between season and initiation local time.

(left) Fig7(a).
Seasonal distribution of detected storms

(right) Fig7(b) ~ (e).
95% confidence interval for the probability of dust storm occurrence in each seasons

(below) Table2.
Local time dependency of dust storm initiation from Fig7 (b) ~ (e)

Southern Season	Local time dependency
Summer, Fall	Not clear
Winter	1200LT
Spring	0900LT

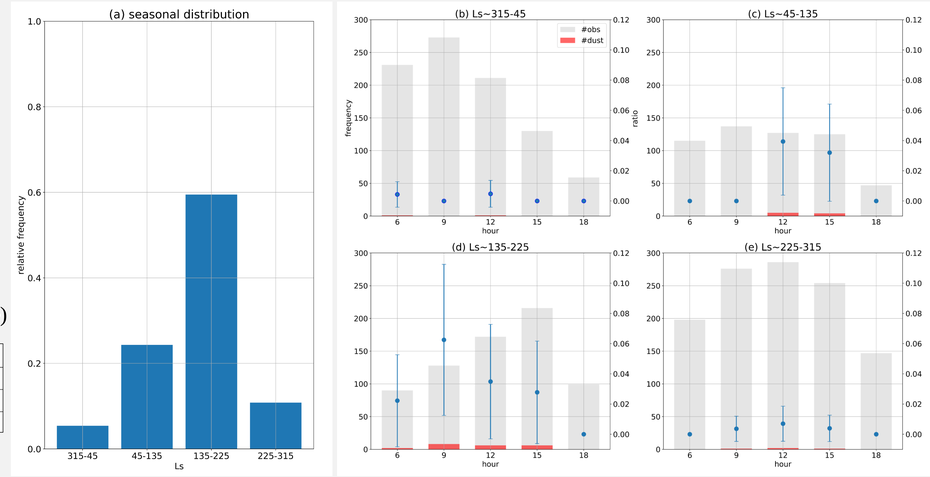

Then, we calculated the ratio of the occurrence time in all observed images at local time X and the 95% confidence interval to see the local time dependency. The ratio $\hat{p}$ is given as $\hat{p} = x/n$, where n is the total number of observations in the local time (gray bar in Fig7 (b) ~ (e)), and x is the number of dust storms (red bar in Fig7 (b) ~ (e)). 95% confidence interval is given as follows:

$$\hat{p} - Z_{0.025}\sqrt{\frac{\hat{p}(1-\hat{p})}{n}} < p < \hat{p} + Z_{0.025}\sqrt{\frac{\hat{p}(1-\hat{p})}{n}}$$

The results are displayed in Fig7(b) ~ (e). They suggest that it is likely to occur frequently around 1200LT in the southern winter, and 0900LT in southern spring. On the contrary, we cannot see it in the southern summer and fall due to the small number of storms (Table2).

4. References

[1] Battalio, M., Wang, H., 2019. The Aonia-Solis-Valles dust storm track in the southern hemisphere of Mars. Icarus 321, 367-378.
[2] Almatroushi, H., AlMazmi, H., AlMheiri, N., AlShamsi, M., AlTunaiji, E., Badri, K., et al. (2021). Emirates Mars mission characterization of Mars atmosphere dynamics and processes. Space Science Reviews, 217(8), 89.
[3] Guha, B. K., Gebhardt, C., Young, R. M. B., Wolff, M. J., & Montabone, L. (2024). Seasonal and diurnal variations of dust storms in Martian year 36 based on the EMM-EXI database. Journal of Geophysical Research: Planets, 129, e2023JE008156.
[4] Cantor, B.A., 2007. MOC observations of the 2001 Mars planet-encircling dust storm. Icarus 186 (1), 60–96.
[5] Kulowski, L., Wang, H., Toigo, A.D., 2017. The seasonal and spatial distribution of textured dust storms observed by Mars Global Surveyor Mars Orbiter Camera. Adv. Space Res. 59 (2), 715–721.
[6] Ogohara, K et al., 2011. Automated cloud tracking system for the Akatsuki Venus Climate . Icarus 217, 661-668
[7] Wang, H., Richardson, M.I., 2015. The origin, evolution, and trajectory of large dust storms on Mars during Mars years 24–30 (1999–2011). Icarus 251, 112–127.
[8] Wolff, M.J., Fernando, A., 2022. Diurnal Variations in the Aphelion Cloud Belt as Observed by the Emirates Exploration Imager (EXI). Geophys. Res. 10.1029/2022GL100477